tvst

Comparison of Retinal Nerve Fiber Layer and Ganglion Cell–Inner Plexiform Layer Thickness Values Using Spectral-Domain and Swept-Source OCT

Alessandro Rabiolo[1], Federico Fantaguzzi[1], Giovanni Montesano[2], Maria Brambati[1], Riccardo Sacconi[1], Francesco Gelormini[1], Giacinto Triolo[3], Paolo Bettin[1], Giuseppe Querques[1], and Francesco Bandello[1]

[1] Department of Ophthalmology, University Vita-Salute, IRCCS San Raffaele, Milan, Italy
[2] Optometry and Visual Sciences, City, University of London, London, UK
[3] Ophthalmology Department, Fatebenefratelli and Ophthalmic Hospital, ASST-Fatebenefratelli-Sacco, Milan, Italy

Purpose: To compare peripapillary retinal nerve fiber layer (pRNFL) and macular ganglion cell–inner plexiform layer (mGCIPL) thickness measurements obtained with spectral domain optical coherence tomography (SD-OCT) and swept-source OCT (SS-OCT) using an OCT-angiography scanning protocol, and their ability to distinguish among patients with glaucoma, glaucoma suspects (GS), and healthy controls (HC).

Methods: Cross-sectional study of 196 eyes (81 glaucoma, 48 GS, and 67 HC) of 119 participants. Participants underwent peripapillary and macular OCT with SD-OCT and SS-OCT. Parameters of interest were average and sector-wise pRNFL and mGCIPL thickness. Inter-device agreement was investigated with Bland-Altman statistics. Conversion formulas were developed with linear regression. Diagnostic performances were evaluated with area under the receiver operating characteristic curves.

Results: Both SD-OCT and SS-OCT detected a significant pRNFL and mGCIPL thinning in glaucoma patients compared to HC and GS for almost all study sectors. A strong linear relationship between the two devices was present for all quadrants/sectors ($R^2 \geq 0.81$, $P < 0.001$), except for the nasal ($R^2 = 0.49$, $P < 0.001$) and temporal ($R^2 = 0.62$, $P < 0.001$) pRNFL quadrants. SD-OCT and SS-OCT measurements had a proportional bias, which could be removed with conversion formulas. Overall, the two devices showed similar diagnostic abilities.

Conclusions: Thickness values obtained with SD-OCT and SS-OCT are not directly interchangeable but potentially interconvertible. Both devices have a similar ability to discriminate glaucoma patients from GS and healthy subjects.

Translational Relevance: OCT-Angiography scans can be reliably used to obtain structural metrics in glaucoma patients.

Introduction

Glaucoma is a progressive optic neuropathy characterized by degeneration of retinal ganglion cells and their axons (retinal nerve fibers), which results in typical changes of the optic nerve head (ONH), retinal nerve fiber layer (RNFL), and visual field (VF). Structural optical coherence tomography (OCT) provides accurate measurements of both peripapillary RNFL (pRNFL) and macular ganglion cell-inner plexiform layer (mGCIPL) thickness and, along with VF and disc photography, is an established tool in the management of glaucoma patients.[1]

OCT technology has considerably evolved throughout the past two decades. Time-domain OCT (TD-OCT) was the technology used for the first commercially available device and was subsequently replaced by spectral-domain OCT (SD-OCT). Several studies have shown that peripapillary and macular thick-

ness parameters as calculated by these two technologies are not interchangeable, despite being closely related.[2–7] In their commercial implementations, SD-OCT allows for faster scans and higher resolution compared to TD-OCT. SD-OCT devices have shown greater ability to detect early glaucomatous changes than TD-OCT.[8] Moreover, SD-OCT may better detect structural progression and quantify its rates because of the lower measurement variability.[4]

OCT technology has further advanced with the introduction of swept-source-OCT (SS-OCT), which became available in clinical practice in 2012. SS-OCT has considerably higher scanning speed (∼100 000 A-scans/sec) than SD-OCT (25,000-85,000 A-scans/sec) and relies on longer wavelengths (1060 nm, compared to 840-850 nm of SD-OCT), allowing better visualization of deep structures such as choroid, lamina cribrosa, and sclera. On the other hand, SD-OCT devices have higher axial resolution than SS-OCT, because axial resolution scales with the square of the central wavelength and the inverse of the bandwidth of the applied light source. Thanks to enhanced depth imaging and frame averaging, SD-OCT remains competitive in evaluating deep structures. Because of the longer wavelength, SS-OCT may have less light scattering from inner retinal layers, resulting in a lower signal-to-noise ratio.

A limited number of studies have explored the diagnostic capabilities of SS-OCT in glaucoma and the level of agreement with SD-OCT.[9–11] Most of the studies compared devices from different manufacturers, which have differences in scanning and acquisition protocols, segmentation algorithms, and image processing methods. This limits the ability to understand whether any differences between SD-OCT and SS-OCT are due to the different scanning technology or the device used. Previous studies have shown that measurement values obtained with different SD-OCT devices from different manufacturers are not interchangeable and have both systematic and proportional bias.[7,12–14] To our knowledge, only Tan and colleagues[15] performed a study comparing an SD-OCT and an SS-OCT from the same manufacturer, and they found a good-to-excellent level of agreement between the two devices. This work also showed that OCT-angiography scanning protocols may reliably provide peripapillary vascular and structural data at the same time. The study, however, had several limitations, including the small sample size (especially with regard to glaucoma cohort), lack of information about the macular region, manual and operator-dependent segmentation of pRNFL boundaries for the SS-OCT scans, use of in-house algorithms to post-process SS-OCT raw images, and no information on whether SS-OCT and SD-OCT have similar ability to diagnose glaucoma.

In this study, we provide a comprehensive comparison between SD-OCT using a standard glaucoma acquisition protocol and SS-OCT using an OCT-angiography scanning protocol. We compared peripapillary and macular thickness values obtained with the two devices, estimated clinical dynamic range and measurement floor, evaluated the interdevice agreement and their influencing factors, and tested these two devices' ability to distinguish among patients with glaucoma, suspected glaucoma, and healthy subjects.

Methods

Study Population

In this cross-sectional diagnostic study, we prospectively enrolled patients with glaucoma, suspected glaucoma, and healthy controls (HCs) between September 2016 to August 2019 at the Department of Ophthalmology, San Raffaele Scientific Institute, Milan, Italy. The study adhered to the tenants of the Declaration of Helsinki and was approved by San Raffaele's Hospital Ethics Committee. All participants provided written consent to participate in observational studies. The same cohort of patients and data were used in another publication.[16]

We prospectively identified patients diagnosed with primary open-angle glaucoma or glaucoma suspect (GS) by a glaucoma specialist. Patients meeting the study criteria were invited to enter the study. Patients with glaucoma were defined by the presence of ONH features (e.g., characteristic RNFL defects, neuroretinal rim thinning or notching) at the dilated fundus examination attributed to primary open-angle glaucoma based on a review of all clinical information, as determined by the glaucoma specialist treating the patient. The presence of a VF defect was not strictly required to make a diagnosis of glaucoma. Two investigators (A.R. and F.F.) masked to the diagnosis collegially reviewed all the visual fields during the data analysis phase and determined whether a clinically relevant visual field abnormality attributable to glaucoma was present. All glaucoma patients were found to have evidence of glaucomatous VF defects in at least one study eye. Patients with suspected glaucoma were defined by either ocular hypertension or suspicious-looking ONH (e.g., large ONH cupping with no neuroretinal rim thinning/notching, cup vertical elongation, optic disc hemorrhage with intact neuroretinal rim) in the absence of any glaucomatous VF damage, as determined by the clinician

treating the patient. Ocular hypertension was defined as untreated intraocular pressure > 21 mm Hg in at least two visits six months or more apart. OCT imaging was not used to make a diagnosis of glaucoma or GS. Healthy subjects were recruited in the ophthalmology department among staff members, patients' spouses or friends (not relatives), and patients with no ocular disease who came for refraction only. Healthy subjects had no evidence of glaucomatous damage and were required to have (i) normal-appearing ONH with intact rim, intact RNFL, and intereye vertical cup-to-disc ratio asymmetry <0.2; (ii) normal VF with glaucoma hemifield test within normal limits, and (iii) intraocular pressure ≤ 21 mm Hg. Regardless of the group, all patients were required to fulfil the following study inclusion criteria: age equal to 18 years or greater; open angles on gonioscopy, defined as trabecular meshwork visible for >180°; spherical equivalent between −6 and +3 diopters. Common exclusion criteria were any other ocular disease or any systemic disease potentially affecting OCT imaging; media opacity or poor fixation preventing adequate image acquisition; and previous intraocular surgery except uneventful cataract surgery >6 months before enrollment in the study. Each participant was assigned to a diagnostic category based on the status of the worse eye; both eyes of the same patient were included if study criteria were met.

All patients underwent comprehensive examination including dynamic gonioscopy, Goldmann applanation tonometry, pachymetry, dilated fundus examination, Humphrey VF using 30-2 grid, stimulus III, SITA-standard algorithm, spectral-domain OCT (Cirrus HD-OCT 5000; Zeiss, Dublin, CA, USA) and swept-source OCT-A (PLEX Elite 9000; Zeiss). OCT scans were acquired after pupil dilation. Two investigators (A.R., F.F.) reviewed all OCT images collegially, excluding those with poor centration, segmentation failure, and artifacts (e.g., motion, blinking).

Spectral-Domain OCT

Peripapillary (optic disc 200 × 200 cube) and macular (macular 512 × 128 cube) scans were acquired with the Cirrus HD-OCT 5000 to obtain pRNFL and mGCIPL thickness values, respectively. For the peripapillary scans, average and quadrant-wise pRNFL thicknesses were extracted. For the macular scans, average, minimum, and sector-wise mGCIPL thickness values were obtained.

Swept-Source OCT

Peripapillary and macular 6 × 6 mm cubes centered on the ONH and fovea were acquired with the PLEX Elite 9000 device. Anonymized raw data were exported and uploaded in the Advanced Retina Imaging Network Hub (https://arinetworkhub.com), a cloud collaboration platform providing access to its members to a wide range of prototype research algorithms to analyze images acquired with the PLEX Elite 9000 device. Peripapillary and macular cubes were analyzed using the Nerve Fiber Layer Microvasculature Density v0.9 and Superficial and GCIPL analysis v0.3 algorithms, respectively. These are early prototype algorithms developed by Zeiss.[17,18] Because these are prototype algorithms, we carefully reviewed all output images and values for accuracy of the analysis. For the peripapillary scans, average and quadrant-wise pRNFL thicknesses were extracted. For the macular scans, average and sector-wise mGCIPL thickness values were obtained.

Statistical Analysis

Statistical analysis was performed with the open-source software R (R Foundation for Statistical Computing, Vienna, Austria). All tests were two-tailed, and *P* values <0.05 were considered statistically significant. For continuous variables, frequency histograms and quantile-quantile plots were visually inspected to determine the distribution (Gaussian vs. non-Gaussian). Continuous Gaussian and non-Gaussian variables were reported as mean (± standard deviation [SD]) and median (interquartile range), respectively; discrete variables were reported as frequencies and proportions.

Differences in patient-related demographic and clinical variables among patients with glaucoma, GSs, and HCs were tested with analysis of variance with Tukey post-hoc test and χ^2 for continuous and categorical variables, respectively. Differences for eye-related variables among the three groups were tested with linear mixed models, which are extensions of traditional linear models and allow us to account for correlated observations, such as the inclusion of two eyes of the same subject. In our models, the patient identification number was the random effect term to account for within-subject correlations because of the inclusion of two eyes of the same patient. Differences in pRNFL and mGCIPL thickness values among the three groups as a function of the OCT device were investigated with linear mixed models. In these models, peripapillary or macular thickness values were the outcome variable, the diagnostic status was the fixed factor along with the patients' age and device signal strength (SS) to account for differences in these variables among the groups, and the patient ID was the random effect term to account for the inclusion of both eyes of the same patient.

Potential factors associated with the absolute difference in thickness values between the two OCT devices were investigated with linear mixed models. The following covariates were screened: age, gender, diagnostic status (i.e., glaucoma, GS, HC), averaged thickness values and SS between the two devices, the difference in SS between the two devices, scan location (i.e., peripapillary, macula), and disc area. Variables to enter in the final model were selected with the least absolute shrinkage and selection operator (LASSO) regression. LASSO is a form of penalized linear regression that shrinks some coefficients' magnitude and sets others to zero; non-zero coefficients were kept into the final model. Variables selected by LASSO regression were entered as fixed factors in the multivariable model, whereas the patient and eye identification number were the outer and inner random effect term to account for within-subject (two eyes of the same patient) and within-eye (multiple quadrants/sectors from the same OCT scan belonging to the same eye) correlations.

Univariable linear regression between thickness values as measured by the two OCT instruments was performed for each pair of quadrants. Bivariate plots were visually inspected to assess the degree and pattern of relationships, and coefficients of determination (R^2) and P values were used to summarize the strength of linear relationships. Bland-Altman statistics and plots were used to investigate the agreement between the two devices. Calibration equations between the two OCT devices for each of the measures of interest were calculated with linear regression.

Diagnostic abilities to distinguish between (1) glaucoma patients and HCs and (2) glaucoma patients and GSs were evaluated with sensitivity at 90% specificity and area under the receiver operating characteristic (AUROC). ROC curves illustrate the relationship between clinical sensitivity and false-positive rate (1-specificity) for every continuous value measured by instruments. On the other hand, sensitivities at fixed specificity provide pointwise information as they inform on a single point of the ROC curve, corresponding to one specific cutoff value. Age- and SS-adjusted pRNFL and mGCIPL values were used to build the ROC curves and estimate sensitivity at 90% specificity, using a method similar to previous studies.[16,19,20] Briefly, a linear mixed model was fit on healthy eyes to calculate normative values for age, SS, and sector. For patients with glaucoma and suspected glaucoma, the normative models were calculated from all HCs. For HCs, normative values were estimated using a twofold cross-validation design, where the dataset of healthy eyes was randomly split into two halves, and each half was used to estimate normative equations for the other half. Because a separate dataset of healthy eyes was not available, the twofold cross-validation avoids using the same eye both for parameter estimation and prediction. For each eye and sector of interest, we predicted age and SS normative values using the normative equations, and we calculate the difference between the observed and normative values. This differential value represents how much the measured thickness in a given eye deviates from the expected value in a healthy subject of the same age and with the same image quality. Differential values between observed and normative data were used to build the ROC curve and calculate sensitivities at 90% specificity. By doing so, age and SS differences were taken into consideration without using these variables to discriminate among groups. We clustered all the ROC curves for the patient identification number to account for the inclusion of two eyes of the same patient, obtain unbiased 95% confidence intervals, and test pairwise differences, as proposed by Obuchowski.[21]

A within-study clinical dynamic range of the two instruments was estimated for each parameter of interest. The dynamic range represents the range of smallest and largest values that an instrument can measure, and it was calculated as the difference between the ninety-fifth percentiles of thickness in HCs and the fifth percentile in glaucoma patients. We chose to use the 5-95% range, and not the full range (min and max values), to limit the effect of potential outliers.

Results

Two hundred twenty-three eyes of 142 participants were enrolled. Of those, 27 eyes of 23 patients were excluded because of poor image quality, poor centration, segmentation failure, and artifacts. The remaining 196 eyes (81 glaucoma, 48 GS, and 67 HC) of 119 participants were included in the study. Table 1 illustrates demographic and main clinical characteristics. Glaucoma patients (62.8 ± 13.5 years) were significantly older than GSs (50.2 ± 15.3 years, $P < 0.001$) and HCs (50.3 ± 14.4 years, $P < 0.001$). Most glaucoma patients had mild-to-moderate VF damage with a median (interquartile range) mean deviation of −3.3 (−6.5 to −1.4) dB. At the peripapillary scans, glaucoma patients had lower SS than HCs with both Cirrus HD-OCT ($P = 0.011$) and PLEX Elite 9000 ($P = 0.026$), whereas GSs had lower SS than HCs with PLEX Elite 9000 ($P = 0.005$) but not with Cirrus HD-OCT ($P = 0.55$). No difference in SS among groups was seen for macular scans.

Peripapillary RNFL thickness values as a function of the OCT device are illustrated in Figure 1 and

Table 1. Demographic and Main Clinical Data of Patient Cohort

| Parameters	Glaucoma	GS	HC	P Value	Glaucoma vs HC	Glaucoma vs GS	GS vs HC
No. Patients/Eyes	52/81	29/48	38/67				
Age (y)	62.8 ± 13.5	50.2 ± 15.3	50.3 ± 14.4	**<0.001**	**<0.001**	**<0.001**	1
Ethnicity, Caucasian	52	29	38				
Sex, male/female				0.34			
Male	20	16	16				
Female	32	13	22				
Eye, right/left							
Right	40	23	34				
Left	41	25	33				
Cirrus HD-OCTSS Peripapillary, mean ± SD	7.5 ± 1.4	7.8 ± 1.1	8.0 ± 1.0	**0.011**	**0.011**	0.26	0.55
PLEX Elite 9000SS Peripapillary, mean ± SD	8.1 ± 1.0	7.9 ± 0.8	8.6 ± 0.8	**0.004**	**0.026**	0.55	**0.005**
Cirrus HD-OCTSS Macula, mean ± SD	8.0 ± 1.4	8.5 ± 1.1	8.4 ± 1.1	0.14			
PLEX Elite 9000SS Macula, mean ± SD	8.4 ± 0.9	8.2 ± 0.8	8.7 ± 1.0	0.13			
Visual Field MD, dB, median [IQR]	−3.3[−6.5 to −1.4]	−1.2[−2.5 to −0.1]	0.0[−3.0 to 0.9]	**0.001**	**0.013**	**0.030**	0.67
Disc area (mm²), mean ± SD	1.9 ± 0.4	1.9 ± 0.4	1.9 ± 0.3	0.72			
Rim area (mm²), mean ± SD	0.9 ± 0.3	1.1 ± 0.2	1.4 ± 0.3	**<0.001**	**<0.001**	**<0.001**	**<0.001**

IQR, interquartile range; MD, mean deviation; SS, signal strength.
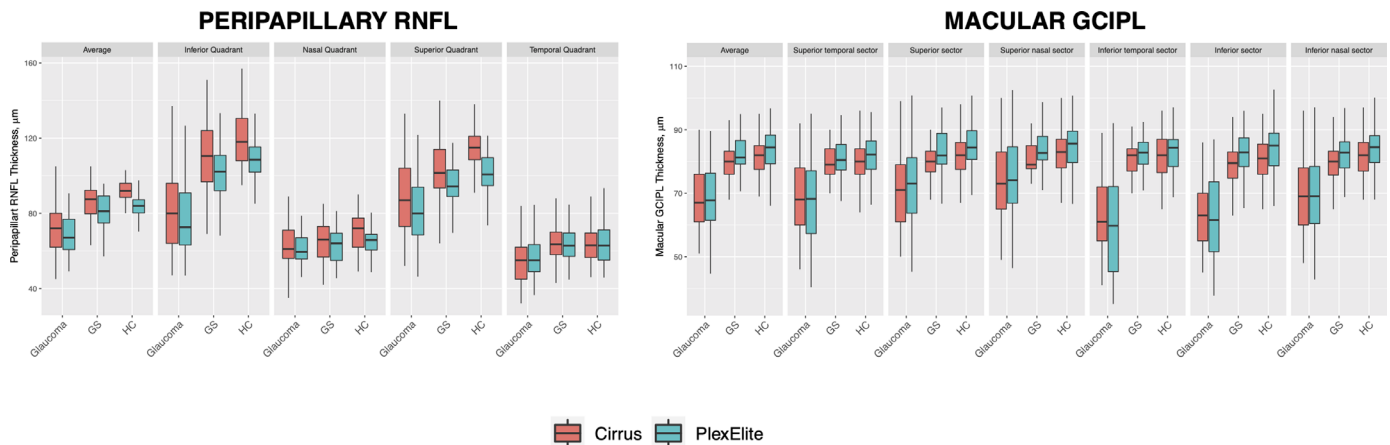
Figure 1. Peripapillary RNFL thickness (**left panel**) and macular GCIPL thickness (**right panel**) values among patients with glaucoma, suspected glaucoma (GS), and HC as a function of the OCT device.

detailed in Supplementary Table S1. Regardless of the OCT device, glaucoma patients had lower peripapillary pRNFL thickness values than HCs at all quadrants but the temporal one ($P = 0.05$ and $P = 0.09$ for Cirrus HD-OCT and PLEX Elite 9000, respectively). Similarly, glaucoma patients had lower peripapillary pRNFL thickness values than GSs with both devices for all quadrants, except for the nasal ($P = 0.72$ and $P = 0.83$ for Cirrus HD-OCT and PLEX Elite 9000, respectively) and temporal ($P = 0.77$ for PLEX Elite 9000) quadrants. Macular GCIPL thickness values obtained with the two OCT devices are illustrated in Figure 1 and detailed in Supplementary Table S2. Glaucoma patients had significantly lower mGCIPL thickness values than both HCs and GSs for all sectors.

Figures 2 and 3, respectively, show the bivariate plots and Bland-Altman plots for peripapillary and macular measurements. Overall, the measurements obtained with the two OCT devices followed a strong linear relationship for all quadrants/sectors ($R^2 \geq 0.81$, $P < 0.001$), except for the nasal ($R^2 = 0.49$, $P < 0.001$) and, to a lesser extent, temporal ($R^2 = 0.62$, $P < 0.001$) pRNFL quadrants. Macular measurements had generally a stronger linear relationship than peripapillary ones ($R^2 \geq 0.85$, $P < 0.001$). The patterns of relationship between the two devices differed for peripapillary and macular measurements. A proportional bias between the two instruments was present, except for the temporal pRNFL quadrant (Fig. 3). The relationship between differences in thickness between
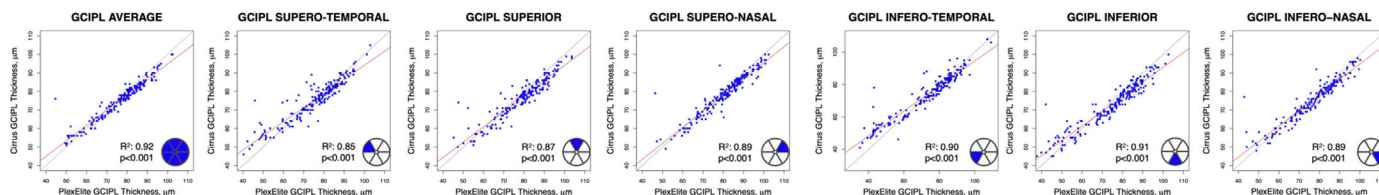
PERIPAPILLARY RNFL
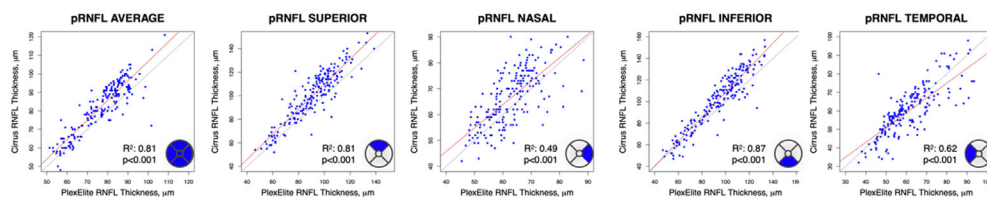
MACULAR GCIPL

Figure 2. Bivariate plots of Cirrus-OCT and PLEXElite 9000 peripapillary RNFL thickness (**top row**) and macular GCIPL thickness **(bottom row)** values. *Solid red* and *black lines* indicate regression and equivalence lines, respectively.

PERIPAPILLARY RNFL
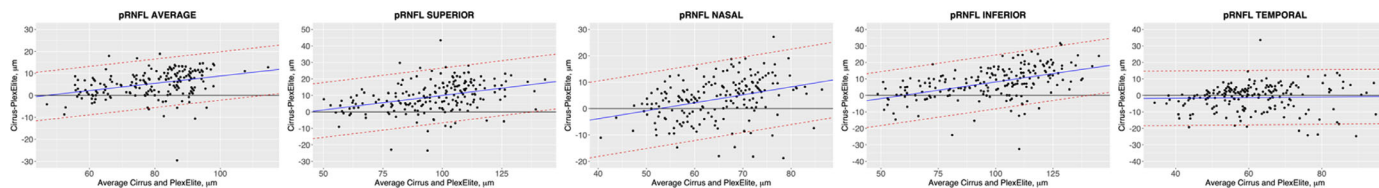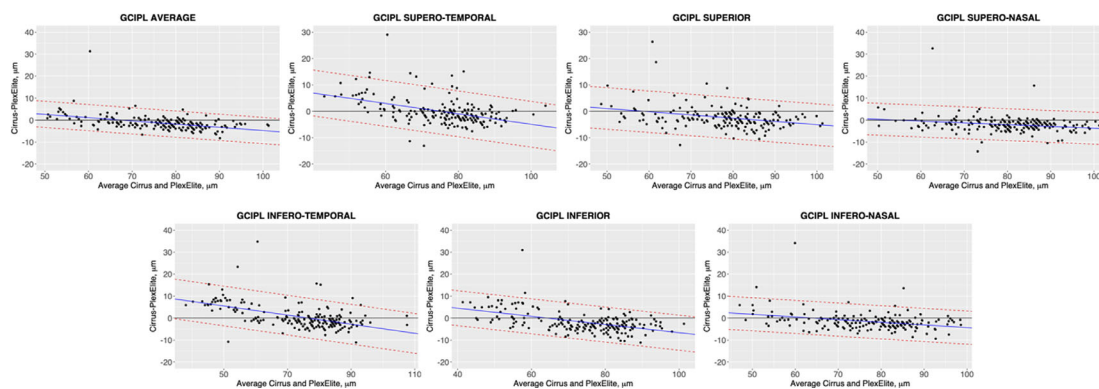
MACULAR GCIPL

Figure 3. Bland-Altman plots of agreement for peripapillary RNFL thickness (**top panel**) and macular GCIPL thickness **(bottom panel)** values. *Black solid line* indicates the no difference line. *Solid blue* and *dashed lines* represent the mean difference and 95% limits of agreements adjusted for the non-uniform differences, respectively.

the two instruments and their mean values was non-uniform and varied as a function of the mean values. For the peripapillary area, Cirrus HD-OCT measurements were generally higher than PLEX Elite 9000 ones, and the discrepancy between the two instruments increased for higher pRNFL thickness values.

For all macular measures, a variable proportional bias was seen with Cirrus HD-OCT and PLEX Elite 9000 leading to higher thickness values in eyes with lower and higher mGCIPL thickness, respectively. A systematic bias existed indicating that the two devices are not directly interchangeable; when the proportional

Table 2. Agreement Between Measurement Obtained With Two OCT Devices According to Bland-Altman Analysis

Parameters	Unadjusted for Nonuniform Differences		Unbiased	
	MD	LoA	MD	LoA
Peripapillary RNFL				
Average	5.4	−6.3/17.2	0.0	−11.0/11.0
Superior quadrant	9.2	−8.6/27.1	0.0	−16.7/16.7
Nasal quadrant	3.6	−11.6/18.8	0.0	−14.3/14.3
Inferior quadrant	7.7	−11.2/26.5	0.0	−16.4/16.4
Temporal quadrant	−1.3	−17.9/15.2	0.0	−16.6/16.6
Macular GCIPL				
Average	−1.3	−8.0/5.5	0.0	−6.0/6.0
Superotemporal	−0.1	−9.8/9.7	0.0	−8.7/8.7
Superior	−2.3	−10.6/6.0	0.0	−7.9/7.9
Superonasal	−2.0	−9.5/5.4	0.0	−7.3/7.3
Inferotemporal	0.6	−10.2/11.3	0.0	−9.0/9.0
Inferior	−1.8	−11.1/7.5	0.0	−8.0/8.0
Inferonasal	−1.6	−9.6/6.5	0.0	−7.5/7.5

LoA, limits of agreement; MD, mean difference.

bias was removed, however, the mean difference was no longer present (Table 2 and Supplementary Figure S1). Calibration equations to convert measurements from Cirrus HD-OCT to PLEX Elite 9000 and vice versa are given in Supplementary Table S3.

Variables selected by the LASSO regression to enter as covariates into the multivariable model for factors associated with the absolute difference in thickness values between the two OCT devices were: baseline thickness, SS difference between the two devices, scan location (i.e., peripapillary, macula), and disc area. In the final multivariable model, greater thickness value (estimate [standard error {SE}] = 1.0 [0.1] μm for every 10 μm increase, $P < 0.001$) and peripapillary scans (estimate [SE] = 4.4 [0.2] μm vs. macular scans, $P < 0.001$) were significantly associated with increased interdevice absolute difference, whereas the SS difference between the two devices (estimate [SE] = 0.1 [0.1] μm for each unit increase, $P = 0.46$) and the disc area (estimate [SE] = 0.5 [0.5] μm vs. macular scans, $P = 0.36$) were not.

Table 3 illustrates the within-study clinical dynamic range of Cirrus-HD and PLEX Elite 9000. For the peripapillary area, Cirrus-HD had a wider pRNFL dynamic range than PLEX Elite 9000 at all quadrants, but its measurement floor was lower than PLEX Elite 9000 only for temporal and nasal quadrants. On the other hand, PLEX Elite 9000 had a wider mGCIPL dynamic range and lower measurement floor than Cirrus-HD at all macular sectors.

Table 3. Clinical Dynamic Range of the Two OCT Devices

Parameters	Dynamic Range (5th – 95th Percentiles), μm	
	Cirrus HD-OCT	PLEX Elite 9000
Peripapillary RNFL		
Average	45 (57–102)	41 (55–96)
Superior quadrant	80 (56–136)	70 (50–120)
Nasal quadrant	48 (38–86)	28 (48–76)
Inferior quadrant	92 (52–144)	79 (51–130)
Temporal quadrant	51 (35–86)	45 (40–85)
Macular GCIPL		
Average	39 (55–94)	45 (51–96)
Superotemporal	46 (48–94)	52 (43–95)
Superior	44 (52–96)	50 (48–98)
Superonasal	43 (52–95)	49 (49–98)
Inferotemporal	52 (43–95)	57 (38–95)
Inferior	46 (47–93)	56 (40–96)
Inferonasal	45 (50–95)	51 (46–97)

Diagnostic abilities of peripapillary pRNFL and macular mGCIPL obtained with the two OCT devices are illustrated in Figures 4 and 5, respectively, and detailed in Supplementary Table S4. Overall, the two OCT devices had similar diagnostic ability to discriminate between glaucoma patients and HCs, except for the superior macular mGCIPL sector, where Cirrus HD-OCT had higher discrimination than PLEX Elite 9000 (AUROC: 0.764 vs. 0.709, $P = 0.001$). Similarly, the two devices had similar discrimination between patients with glaucoma and those with suspected

translational vision science & technology

Figure 4. ROC curves of pRNFL to discriminate between glaucoma patients and either HCs **(top row)** or GSs **(bottom row)**. *Vertical dotted lines* indicate a value of one-specificity of 0.1.

glaucoma, except for temporal pRNFL quadrant, where Cirrus HD-OCT had higher discrimination than PLEX Elite 9000 (AUROC: 0.687 vs. 0.606, $P = 0.001$), and for the superior pRNFL quadrant, where Cirrus HD-OCT had lower discrimination than PLEX Elite 9000 (AUROC: 0.718 vs. 0.778, $P = 0.044$). Similar results were obtained for sensitivities at 90% specificity (Table 4).
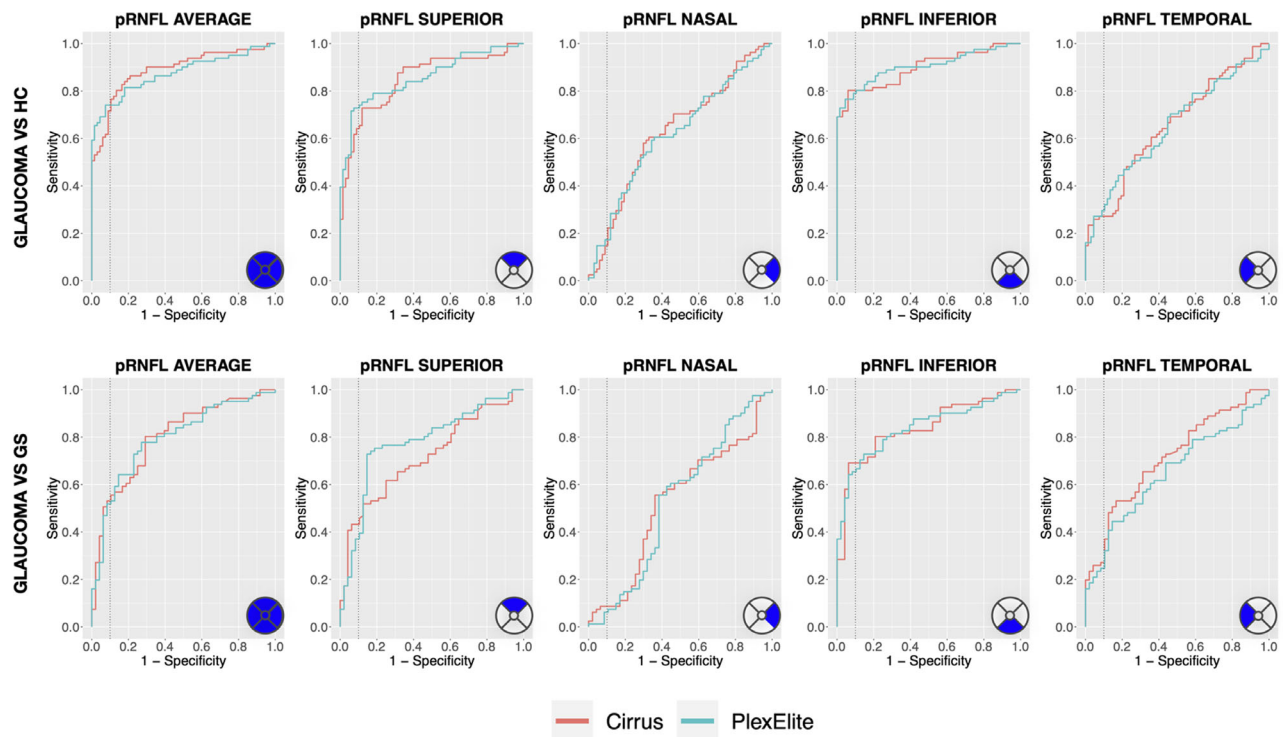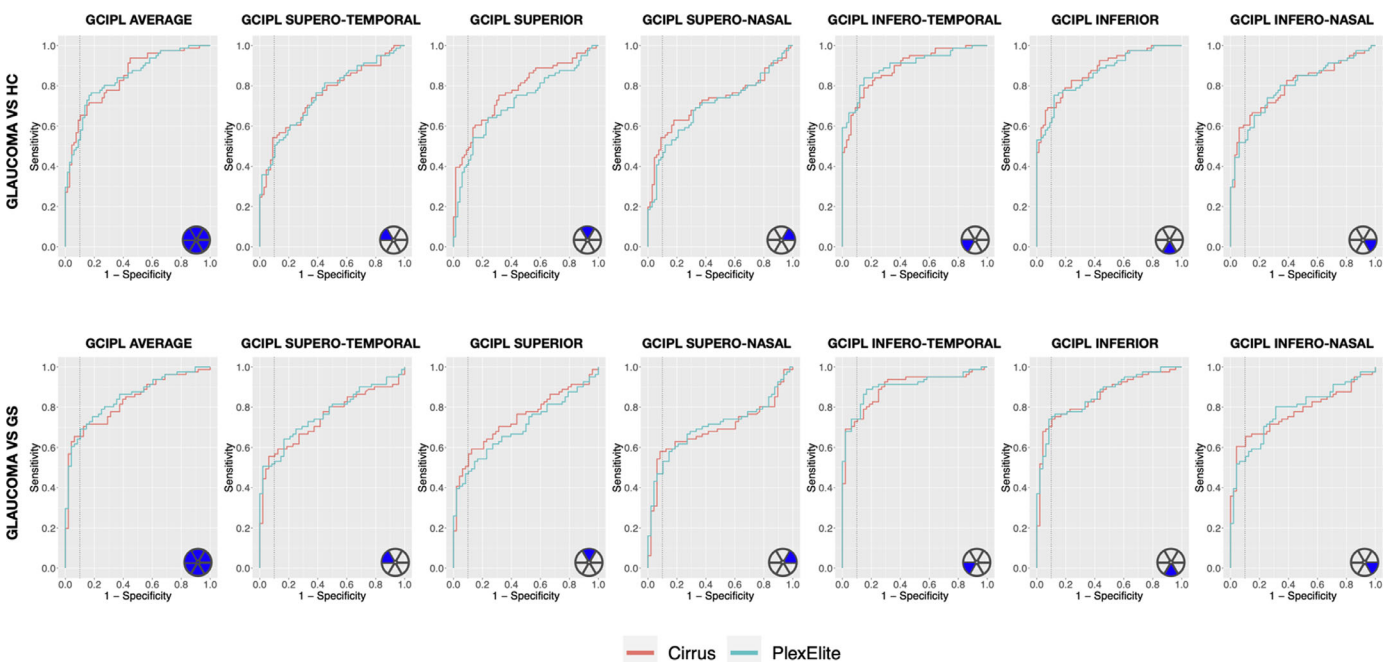

Figure 5. ROC curves of macular GCIPL to discriminate between glaucoma patients and either HCs **(top row)** or GSs **(bottom row)**. *Vertical dotted lines* indicate a value of one-specificity of 0.1.

Table 4.   Sensitivities at 90% Fixed Specificity

	Glaucoma vs HC		Glaucoma vs GS	
Parameters	Cirrus HD-OCT	PLEX Elite 9000	Cirrus HD-OCT	PLEX Elite 9000
Peripapillary				
Average	76.5%	74.1%	56.8%	53.1%
Superior quadrant	65.4%	74.1%	51.9%	39.5%
Nasal quadrant	22.2%	17.3%	4.9%	7.4%
Inferior quadrant	80.2%	80.2%	71.6%	66.7%
Temporal quadrant	27.2%	32.1%	25.9%	32.1%
Macula				
Average	65.4%	58.0%	65.4%	69.1%
Superotemporal	54.3%	50.6%	56.8%	53.1%
Superior	49.4%	43.2%	56.8%	48.1%
Superonasal	54.3%	46.9%	58.0%	53.1%
Inferotemporal	69.1%	71.6%	74.1%	74.1%
Inferior	69.1%	64.2%	74.1%	75.3%
Inferonasal	60.5%	53.1%	65.4%	55.6%

Discussion

In this study, we compared the pRNFL and mGCIPL thickness values as measured with an SD-OCT and an SS-OCT device, tested the interdevice agreement, and their diagnostic ability in a cohort of patients with glaucoma, GSs, and HCs. We found that thickness values as measured with the two devices agreed well with each other, although their absolute values were not directly interchangeable due to the presence of proportional measurement bias. Both devices had a similar ability to discriminate among glaucoma patients, GSs, and HCs.

The pRNFL and mGCIPL thickness measurements are established OCT parameters in the diagnosis of glaucoma.[1] Cirrus HD-OCT is a widely used SD-OCT device, demonstrating high precision and diagnostic accuracy in many studies.[2–4,7,22] PLEX Elite 9000 was mainly developed as an SS-OCT-Angiography platform, but B-scans can be processed to obtain structural metrics, including pRNFL and mGCIPL thicknesses. Hence, PLEX Elite 9000 angiocubes may provide both structural and vascular information with the same acquisition. Although the role of structural parameters in the glaucoma management is established, that of vascular parameters is a matter of controversy, with contrasting results reported in the literature.[16,23–26] In a recent study conducted on the same cohort of patients of this study,[16] we compared the ability of peripapillary and macular structural parameters, vascular parameters, and their integra-

tion to discriminate among patients with glaucoma, suspected glaucoma, and HCs. We found that vascular OCT-angiography did not add additional benefit to structural OCT for the diagnosis of early to moderate glaucoma. Recent studies[27,28] seem to suggest that OCT-angiography may be helpful for the longitudinal monitoring of glaucoma patients, but further research is required to fully elucidate the role of vascular parameters for glaucoma progression. The results of our study, which show that both structural and vascular data can be reliably estimated from the same angiocube, provide useful foundational methodological work for researchers working in the field of OCT-angiography in glaucoma, as well as other ocular conditions, including optic nerve disorders and retinal diseases (e.g., diabetic retinopathy).

The use of SS-OCT in glaucoma has potential advantages. It allows for more rapid image acquisition and potentially larger volumes, imaging macular and optic nerve regions with a single scan. This differs from most SD-OCTs, which require two separate acquisitions centered on the ONH and the fovea to obtain pRNFL and mGCIPL thickness measurements, respectively. Previous studies conducted with a SS-OCT device (different from the one used in this study) have shown that SS-OCT wide-field maps perform equally or better than smaller SD-OCT scans in diagnosing glaucoma and detecting structural progression.[11,29–31] Although the SS-OCT device in this study is able to image wide areas (12 × 12 mm or 15 × 9 mm), these larger scans were developed mainly to obtain vascular OCT-angiography images, and the reliability

and diagnostic ability of structural metrics derived from such larger scans in glaucoma patients are still uncertain. SS-OCT improves the resolution of deeper ocular structures, such as the lamina cribrosa, which has been theorized to be the primary site of axonal damage in glaucoma.[32] Nevertheless, SS-OCT technology does not come without potential drawbacks. Its axial resolution is lower than that of SD-OCTs (PLEX Elite 9000 = 6.3 μm vs. Cirrus HD-OCT = 5 μm), potentially affecting the measurement of inner retinal layers thickness.

Regardless of the device used, we found that average and pRNFL thickness values at all quadrants were significantly lower in glaucoma patients than in HCs. Glaucoma patients had significantly lower pRNFL thickness values than GSs for the average, superior, and inferior quadrants. Glaucoma patients also had significantly lower macular GCIPL thickness for all the selected sectors than HCs and GS. Peripapillary RNFL thickness values as measured by Cirrus HD-OCT and PLEX Elite 9000 had a strong linear relationship in the average, superior, and inferior quadrants. Conversely, the strength of linear relationship for temporal and, especially, nasal peripapillary RNFL quadrants were considerably lower. This is not unexpected because nasal and temporal quadrants are known to have higher test-retest variability and reduced precision than superior and inferior quadrants.[3,5,33] Macular GCIPL thickness values obtained with the two instruments had an excellent degree of linear relationship for all the study sectors. This is not surprising because macular measurements are known to have high reproducibility.[34,35] Our finding is in agreement with the existing literature comparing Cirrus HD-OCT with SS-OCT. Tan et al.[15] compared pRNFL measurements obtained with the same pair of devices used in this study in a small cohort of patients and found strong correlations between measurements obtained with SD-OCT and SS-OCT, except for the nasal quadrant, where the correlation was weak. The study, however, had several limitations, preventing its generalizability. The study relied on a small cohort, especially regarding the number of glaucomatous eyes (12 eyes), with only five eyes having moderate-to-severe glaucoma. The authors did not provide complete information about the relationship between the two instruments across the entire clinically measurable dynamic range, especially for thinner thickness values, which have higher variability and are more prone to segmentation errors.[36] In our study, we found that the measurement difference was not constant along the entire peripapillary RNFL thickness spectrum, and the discrepancy between the two instruments decreased as the RNFL thickness decreased. The study by Tan and colleagues[15] provides no information about the relationship between the two devices for macular GCIPL thickness, which is a valid complement to peripapillary RNFL thickness in glaucoma management. Other comparative studies[9,10] used different pairs of SD-OCT and SS-OCT devices, and none of them used the PLEX Elite 9000 as an SS-OCT. Although their results are in general agreement with ours, they might not be directly generalizable and comparable.

The two devices had variable limits of agreement within their clinical dynamic range with a clear proportional bias. For pRNFL, Cirrus HD-OCT provided higher pRNFL thickness values than PLEX Elite in the thicker end of the dynamic range, whereas measurements tended to converge toward thinner measurements. Macular GCIPL limits of agreement were tighter, and the relationship between the two devices was more complex. Cirrus HD-OCT generally measured higher and lower mGCIPL values than PLEX ELITE 9000 in the thinner and thicker part of the dynamic range, respectively. Tan et al.[15] compared pRNFL thickness as measured by the same pair of devices and same acquisition scans used in our study and found a proportional bias between SD-OCT and SS-OCT, with the discrepancy between the two instruments increasing as the peripapillary RNFL thickness increased but, in contrast with our results, SS-OCT provided higher measurement values than SD-OCT. Several factors may explain such a discrepancy. Tan and colleagues[15] used the automatic segmentation algorithm for Cirrus HD-OCT, whereas a single grader performed a manual segmentation for all the PLEX Elite 9000 images. Manual segmentation allows for greater overall accuracy but is more prone to the introduction of operator-related systematic errors. In our study, the segmentation algorithm was fully automatic for both devices. The authors calculated the peripapillary RNFL thickness with SS-OCT as the average of three circles at 3.44 mm, 3.46 mm, and 3.48 mm diameters from the optic disc center, whereas peripapillary SD-OCT RNFL thickness was extracted from the 3.46 mm diameter circle. Conversely, we calculated the peripapillary RNFL thickness at a circle at 3.46 mm ONH center for both devices. As previously stated, the limited number of glaucomatous eyes in the study by Tan and colleagues[15] may have limited the ability to characterize relationship between the two devices over the entire clinical dynamic range of the instruments. Other studies have reported a proportional bias between SD-OCT and SS-OCT.[9–11] All these studies compared devices from different manufacturers, with different hardware, acquisition process, segmentation algorithm, and post-processing algorithm. Hence, the comparison

between our results and that of these studies may be arduous.

The two devices had different dynamic ranges, with PLEX Elite 9000 having greater mGCIPL and lower pRNFL clinical dynamic range than Cirrus HD-OCT. The measurement floor was similar between the two devices for peripapillary average, superior, and inferior quadrants, but not for nasal and temporal quadrants; for all macular sectors, PLEX Elite 9000 had a lower measurement floor than Cirrus HD-OCT. Dynamic range and measurement floors are important metrics to evaluate the ability of OCT devices to track glaucomatous progression. At comparable levels of test-retest variability, wider dynamic range and lower measurement floor may allow a better monitoring of glaucomatous structural progression. Because only a single peripapillary and macular scan per eye was available, our study does not report whether the two devices have similar test-retest variability and number of measurable steps within their clinical dynamic range. Hence, we were not able to answer the question of whether both Cirrus HD-OCT and Plex Elite 9000 have similar ability to estimate glaucomatous structural progression.

Although absolute RNFL and GCIPL thickness values obtained with the two devices were not directly interchangeable, we estimated conversion equations to convert measurements from one device to the other. After filtering out the measurement bias, the agreement between the two instruments considerably improved. However, the 95% limits of agreement between the two instruments were considerably higher than those reported by previous test-retest studies.[37] Conversion equations may be helpful both in research setting and clinical practice. In research studies, various centers may have different OCT platforms, and measurements may not be directly comparable. Glaucoma patients should be ideally followed up using the same device over time in clinical practice, but this may not always be feasible. Because of the increasing number of OCT instruments and the fast pace at which they become available in clinical practice, it is not uncommon that patients are followed up with various devices. Glaucoma is a chronic disease whose progression may take place over the course of many years, which often exceeds the life of any instrument. Hence, converting measurements from different manufacturers and generations of devices may improve the longitudinal evaluation of structure over long periods of time.

Both Cirrus HD-OCT and PLEX Elite 9000 demonstrated a similar ability to discriminate glaucoma patients from HCs and suspected glaucoma. These results corroborate other studies' findings comparing different SD-OCT and SS-OCT devices.[9,38,39]

The inferior peripapillary quadrant had the best diagnostic accuracy with both devices, followed by average and superior quadrant. This agrees with previous studies showing that these quadrants are highly informative in the discrimination between glaucoma and HCs.[5,9,10,40–45] Among mGCIPL measurements, the inferotemporal sector showed the highest diagnostic ability, in agreement with previous studies.[5,9,43] Both OCT devices had a better ability to discriminate glaucoma patients from HCs than from GSs.

One well-known problem of glaucoma diagnostic studies is that their reported diagnostic accuracy may not translate when used in clinical practice to identify early glaucoma. Such studies are often based on differentiating perfectly healthy eyes from those with established glaucoma. It is usually relatively easy for glaucoma specialists (and skilled comprehensive ophthalmologists) to distinguish between perfectly healthy individuals and glaucoma patients, especially in the case of moderate-to-severe disease.[46] However, this scenario is uncommon in a glaucoma clinic, because glaucoma specialists are often asked to differentiate patients with glaucoma from those with suspected glaucoma. Our inclusion of a comparison between glaucoma patients and GSs was an attempt to mimic the fringe cases that are commonly encountered in clinical practice. Because there is no perfect reference standard in glaucoma diagnosis, the reader must be aware that the distinction between early glaucoma and GS can be challenging and somewhat arbitrary, especially with cross-sectional data.

Other limitations of this study should be acknowledged. One limitation of this study is related to the inaccuracies of segmentation algorithms. Because neither Cirrus HD-OCT and PLEX Elite 9000 post-processing software allows manual correction of segmentation boundaries, we attempted to address this limitation by reviewing B-scan images and excluding scans with segmentation errors. Despite being from the same manufacturer, the two OCT devices may have differences, especially with regards to their segmentation algorithms and image processing methods. The peripapillary segmentation algorithm used by the SS-OCT was adapted from the one used by the SD-OCT device (TomTec segmentation algorithm). On the other hand, the two instruments used two different segmentation algorithms for macular scans. Acquisition scans were different between the two instruments. Structural measurements were obtained from standard structural OCT protocols for the Cirrus HD-OCT, while they were extracted from 6 × 6 mm angiocubes for and PLEX Elite 9000. Different scanning protocols may theoretically have impacted on the SD versus SS comparison. At the present time, however,

Cirrus built-in software does not allow us to extract structural data from angiocubes; on the other hand, traditional structural scans have not been implemented on PLEX Elite 9000, which has been mainly developed as an OCT-angiography platform. Hence, our study does not answer the questions of whether the differences between the two instruments are solely related to the SD-OCT versus SS-OCT technology, especially for the macular scans, where a difference in the segmentation algorithm was also present. Peripapillary RNFL and macular GCIPL measurements are prone to image magnification in eyes with very long or short axial length.[47] However, we did not perform any magnification correction because the axial length was not among the collected variables. In this study, we partially addressed this issue by excluding eyes with high degree of myopic or hyperopic refraction. A previous study has shown that in eyes in which the axial length did not deviate considerably from average values, axial length correction does not provide any significant benefit.[48] This limitation is likely to affect SD-OCT and SS-OCT equally and therefore does not affect our comparisons. Our results may not be generalizable to patients of ethnicities other than European descent, which was the only ethnicity included in this study. The definition of glaucoma in this study required the presence of clinically detectable structural glaucomatous damage. Both SD-OCT and SS-OCT provide structural measurements, and their true diagnostic ability could be overestimated. However, this limitation is likely to affect both devices equally, and therefore our comparison remains valid. Also, the diagnosis of glaucoma was mainly based on the subjective evaluation of the optic nerve by experienced glaucoma clinicians, and previous studies have shown considerable variability in the ONH interpretation.[49] Diagnostic categories in this study were assigned based on the worst eye, and fellow eyes of patients with primary open-angle glaucoma with no clear evidence of glaucomatous damage were considered as affected by early glaucoma, under the clinical assumption that some disease, at least subclinical, was present. Primary open-angle glaucoma is a bilateral though often asymmetrical condition.[50] Once a diagnosis of primary open-angle glaucoma has been established, we believe that the patient, rather than the eye, should be considered affected by glaucoma and treated accordingly. Previous studies have shown that patients with "unilateral" primary open-angle glaucoma demonstrate RNFL thickness reduction in the apparently unaffected eye.[51,52] Also, patients with visual field damage believed to be unilateral may show bilateral damage when tested with nonconventional perimetric strategies.[53,54] Fellow eyes with no clinical evidence of structural or functional damage were only 11 (13.5%), and results remained unchanged even after their exclusion (data not shown). Age and signal strength were different among our diagnostic categories, and these variables are known to impact structural thickness values.[55,56] We used established statistical techniques to control for the confounder effect of such covariates.[19,57] In this study, we run a considerable number of statistical tests, and this may increase the rate of type I error. Because of the study's exploratory nature, we chose not to adjust *P* values for multiple comparisons.[58]

In conclusion, SD-OCT and SS-OCT have similar abilities to discriminate glaucoma patients from GSs and healthy subjects. Although thickness measurements obtained with the two instruments follow a strong linear relationship, they are not directly interchangeable because of the presence of proportional bias, influenced by pRNFL and mGCIPL thickness values. After removing the proportional bias, a mean difference between the two instruments was no longer present, suggesting measures obtained with either instrument are potentially interconvertible. OCT-angiography scans can be reliably used to obtain both structural and vascular metrics in glaucoma patients. Further studies are required to validate our conversion formula in a separate cohort of patients and test the impact of using both devices in the management of glaucoma patients.

Acknowledgments

Disclosure: **A. Rabiolo,** None; **F. Fantaguzzi,** None; **G. Montesano,** CenterVue Spa (C); **M. Brambati,** None; **R. Sacconi,** None; **F. Gelormini,** None; **G. Triolo,** None; **P. Bettin,** None; **G. Querques,** Zeiss (C), Alimera Sciences (C), Allergan Inc (C), Amgen (C), Bayer Shering-Pharma (C), Heidelberg, KBH (C), LEH Pharma (C), Lumithera (C), Novartis (C), Sandoz (C), Sifi (C), Sooft-Fidea (C); **F. Bandello,** Zeiss (C), Alcon (C), Alimera Sciences (C), Allergan Inc (C), Farmila-Thea (C), Bayer Shering-Pharma (C), Bausch and Lomb (C), Genentech (C), Hoffmann-La-Roche (C), Novagali Pharma (C), Novartis (C), Sanofi-Aventis (C), Thrombogenics (C)

References

1. Tatham AJ, Medeiros FA. Detecting structural progression in glaucoma with optical coherence tomography. *Ophthalmology*. 2017;124:S57–S65.

2. Knight OJ, Chang RT, Feuer WJ, Budenz DL. Comparison of retinal nerve fiber layer measurements using time domain and spectral domain optical coherent tomography. *Ophthalmology*. 2009;116:1271–1277.

3. Vizzeri G, Weinreb RN, Gonzalez-Garcia AO, et al. Agreement between spectral-domain and time-domain OCT for measuring RNFL thickness. *Br J Ophthalmol*. 2009;93:775–781.

4. Leung CK, Cheung CY, Weinreb RN, et al. Retinal nerve fiber layer imaging with spectral-domain optical coherence tomography: a variability and diagnostic performance study. *Ophthalmology*. 2009;116:1257–1263, e1251-1252.

5. Leung CK, Chan WM, Yung WH, et al. Comparison of macular and peripapillary measurements for the detection of glaucoma: an optical coherence tomography study. *Ophthalmology*. 2005;112:391–400.

6. Hood DC, Raza AS, Kay KY, et al. A comparison of retinal nerve fiber layer (RNFL) thickness obtained with frequency and time domain optical coherence tomography (OCT). *Opt Express*. 2009;17:3997–4003.

7. Pierro L, Gagliardi M, Iuliano L, Ambrosi A, Bandello F. Retinal nerve fiber layer thickness reproducibility using seven different OCT instruments. *Invest Ophthalmol Vis Sci*. 2012;53:5912–5920.

8. Jeoung JW, Kim TW, Weinreb RN, Kim SH, Park KH, Kim DM. Diagnostic ability of spectral-domain versus time-domain optical coherence tomography in preperimetric glaucoma. *J Glaucoma*. 2019;23:299–306.

9. Yang Z, Tatham AJ, Weinreb RN, Medeiros FA, Liu T, Zangwill LM. Diagnostic ability of macular ganglion cell inner plexiform layer measurements in glaucoma using swept source and spectral domain optical coherence tomography. *PLoS One*. 2015;10:e0125957.

10. Ha A, Lee SH, Lee EJ, Kim TW. Retinal nerve fiber layer thickness measurement comparison using spectral domain and swept source optical coherence tomography. *Korean J Ophthalmol*. 2016;30:140–147.

11. Lee WJ, Oh S, Kim YK, Jeoung JW, Park KH. Comparison of glaucoma-diagnostic ability between wide-field swept-source OCT retinal nerve fiber layer maps and spectral-domain OCT. *Eye (Lond)*. 2018;32:1483–1492.

12. Faghihi H, Hajizadeh F, Hashemi H, Khabazkhoob M. Agreement of two different spectral domain optical coherence tomography instruments for retinal nerve fiber layer measurements. *J Ophthalmic Vis Res*. 2014;9:31–37.

13. Leite MT, Rao HL, Zangwill LM, Weinreb RN, Medeiros FA. Comparison of the diagnostic accuracies of the Spectralis, Cirrus, and RTVue optical coherence tomography devices in glaucoma. *Ophthalmology*. 2011;118:1334–1339.

14. Pakravan M, Pakbin M, Aghazadehamiri M, Yazdani S, Yaseri M. Peripapillary retinal nerve fiber layer thickness measurement by 2 different spectral domain optical coherence tomography machines. *Eur J Ophthalmol*. 2013;23:289–295.

15. Tan B, Chua J, Harish T, et al. Comparison of a commercial spectral-domain OCT and swept-source OCT based on an angiography scan for measuring circumpapillary retinal nerve fibre layer thickness. *Br J Ophthalmol*. 2020;104:974–979.

16. Rabiolo A, Fantaguzzi F, Sacconi R, et al. Combining structural and vascular parameters to discriminate among glaucoma patients, glaucoma suspects, and healthy subjects. *Transl Vis Sci Technol*. 2021;10:20.

17. Rabiolo A, Gelormini F, Sacconi R, et al. Comparison of methods to quantify macular and peripapillary vessel density in optical coherence tomography angiography. *PLoS One*. 2018;13:e0205773.

18. Ishii H, Shoji T, Yoshikawa Y, Kanno J, Ibuki H, Shinoda K. Automated measurement of the foveal avascular zone in swept-source optical coherence tomography angiography images. *Transl Vis Sci Technol*. 2019;8:28.

19. Montesano G, Rossetti LM, McKendrick AM, et al. Effect of fundus tracking on structure-function relationship in glaucoma. *Br J Ophthalmol*. 2020;104:1710–1716.

20. Hirasawa K, Smith CA, West ME, et al. Discrepancy in loss of macular perfusion density and ganglion cell layer thickness in early glaucoma. *Am J Ophthalmol*. 2021;221:39–47.

21. Obuchowski NA. Nonparametric analysis of clustered ROC curve data. *Biometrics*. 1997;53:567–578.

22. Park SB, Sung KR, Kang SY, Kim KR, Kook MS. Comparison of glaucoma diagnostic capabilities of cirrus HD and stratus optical coherence tomography. *Arch Ophthalmol*. 2009;127:1603–1609.

23. Triolo G, Rabiolo A, Shemonski ND, et al. Optical coherence tomography angiography macular

and peripapillary vessel perfusion density in healthy subjects, glaucoma suspects, and glaucoma patients. *Invest Ophthalmol Vis Sci*. 2017;58:5713–5722.

24. Bowd C, Belghith A, Proudfoot JA, et al. Gradient-boosting classifiers combining vessel density and tissue thickness measurements for classifying early to moderate glaucoma. *Am J Ophthalmol*. 2020;217:131–139.

25. Andrade De Jesus D, Sanchez Brea L, Barbosa Breda J, et al. OCTA multilayer and multisector peripapillary microvascular modeling for diagnosing and staging of glaucoma. *Transl Vis Sci Technol*. 2020;9:58.

26. Kwon HJ, Kwon J, Sung KR. Additive role of optical coherence tomography angiography vessel density measurements in glaucoma diagnoses. *Korean J Ophthalmol*. 2019;33:315–325.

27. Nishida T, Moghimi S, Wu JH, et al. Association of initial optical coherence tomography angiography vessel density loss with faster visual field loss in glaucoma. *JAMA Ophthalmol*. 2022;140(4):319–326.

28. Hou H, Moghimi S, Proudfoot JA, et al. Ganglion cell complex thickness and macular vessel density loss in primary open-angle glaucoma. *Ophthalmology*. 2020;127:1043–1052.

29. Kim YW, Lee J, Kim JS, Park KH. Diagnostic accuracy of wide-field map from swept-source optical coherence tomography for primary open-angle glaucoma in myopic eyes. *Am J Ophthalmol*. 2020;218:182–191.

30. Kim H, Park HM, Jeong HC, et al. Wide-field optical coherence tomography deviation map for early glaucoma detection [Online ahead of print. July 22, 2021]. *Br J Ophthalmol*, doi:10.1136/bjophthalmol-2021-319509.

31. Lee WJ, Seong M, Lim HW, et al.: Re: Wide-field trend-based progression analysis of combined retinal nerve fiber layer and ganglion cell inner plexiform layer thickness (Ophthalmology. 2020;127:1322-1330). *Ophthalmology*. 2021;128:e7–e8.

32. Takusagawa HL, Hoguet A, Junk AK, Nouri-Mahdavi K, Radhakrishnan S, Chen TC. Swept-source OCT for evaluating the lamina cribrosa: a report by the American Academy of Ophthalmology. *Ophthalmology*. 2019;126:1315–1323.

33. Mwanza JC, Chang RT, Budenz DL, et al. Reproducibility of peripapillary retinal nerve fiber layer thickness and optic nerve head parameters measured with cirrus HD-OCT in glaucomatous eyes. *Invest Ophthalmol Vis Sci*. 2010;51:5724–5730.

34. Mwanza JC, Oakley JD, Budenz DL, Chang RT, Knight OJ, Feuer WJ. Macular ganglion cell-inner plexiform layer: automated detection and thickness reproducibility with spectral domain-optical coherence tomography in glaucoma. *Invest Ophthalmol Vis Sci*. 2011;52:8323–8329.

35. Francoz M, Fenolland JR, Giraud JM, et al. Reproducibility of macular ganglion cell-inner plexiform layer thickness measurement with cirrus HD-OCT in normal, hypertensive and glaucomatous eyes. *Br J Ophthalmol*. 2014;98:322–328.

36. Liu Y, Simavli H, Que CJ, et al. Patient characteristics associated with artifacts in Spectralis optical coherence tomography imaging of the retinal nerve fiber layer in glaucoma. *Am J Ophthalmol*. 2015;159:565–576.e562.

37. Wadhwani M, Bali SJ, Satyapal R, et al. Test-retest variability of retinal nerve fiber layer thickness and macular ganglion cell-inner plexiform layer thickness measurements using spectral-domain optical coherence tomography. *J Glaucoma*. 2015;24:e109–115.

38. Lee KM, Lee EJ, Kim TW, Kim H. Comparison of the abilities of SD-OCT and SS-OCT in evaluating the thickness of the macular inner retinal layer for glaucoma diagnosis. *PLoS One*. 2016;11:e0147964.

39. Lee SY, Bae HW, Seong GJ, Kim CY. Diagnostic ability of swept-source and spectral-domain optical coherence tomography for glaucoma. *Yonsei Med J*. 2018;59:887–896.

40. Gyatsho J, Kaushik S, Gupta A, Pandav SS, Ram J. Retinal nerve fiber layer thickness in normal, ocular hypertensive, and glaucomatous Indian eyes: an optical coherence tomography study. *J Glaucoma*. 2008;17:122–127.

41. Medeiros FA, Zangwill LM, Bowd C, Vessani RM, Susanna R, Jr., Weinreb RN. Evaluation of retinal nerve fiber layer, optic nerve head, and macular thickness measurements for glaucoma detection using optical coherence tomography. *Am J Ophthalmol*. 2005;139:44–55.

42. Mwanza JC, Oakley JD, Budenz DL, Anderson DR, Cirrus Optical Coherence Tomography Normative Database Study G. Ability of cirrus HD-OCT optic nerve head parameters to discriminate normal from glaucomatous eyes. *Ophthalmology*. 2011;118:241–248.e241.

43. Mwanza JC, Durbin MK, Budenz DL, et al. Glaucoma diagnostic accuracy of ganglion cell-inner plexiform layer thickness: comparison with nerve fiber layer and optic nerve head. *Ophthalmology*. 2012;119:1151–1158.

44. Wollstein G, Schuman JS, Price LL, et al. Optical coherence tomography longitudinal evaluation of retinal nerve fiber layer thickness in glaucoma. *Arch Ophthalmol*. 2005;123:464–470.

45. Yuksel N, Altintas O, Ozkan B, Karadag S, Caglar Y. Discriminating ability of optical coherence tomography data in staging glaucomatous damage. *Can J Ophthalmol*. 2009;44:297–307.

46. Bussel II, Wollstein G, Schuman JS. OCT for glaucoma diagnosis, screening and detection of glaucoma progression. *Br J Ophthalmol*. 2014;98(Suppl 2):ii15–ii19.

47. Kang SH, Hong SW, Im SK, Lee SH, Ahn MD. Effect of myopia on the thickness of the retinal nerve fiber layer measured by Cirrus HD optical coherence tomography. *Invest Ophthalmol Vis Sci*. 2010;51:4075–4083.

48. Nowroozizadeh S, Cirineo N, Amini N, et al. Influence of correction of ocular magnification on spectral-domain OCT retinal nerve fiber layer measurement variability and performance. *Invest Ophthalmol Vis Sci*. 2014;55:3439–3446.

49. Zeyen T, Miglior S, Pfeiffer N, Cunha-Vaz J, Adamsons I, European Glaucoma Prevention Study G. Reproducibility of evaluation of optic disc change for glaucoma with stereo optic disc photographs. *Ophthalmology*. 2003;110:340–344.

50. Gedde SJ, Vinod K, Wright MM, et al. Primary open-angle glaucoma preferred practice pattern. *Ophthalmology*. 2021;128:P71–P150.

51. Bertuzzi F, Hoffman DC, De Fonseka AM, Souza C, Caprioli J. Concordance of retinal nerve fiber layer defects between fellow eyes of glaucoma patients measured by optical coherence tomography. *Am J Ophthalmol*. 2009;148:148–154.

52. Kim DM, Hwang US, Park KH, Kim SH. Retinal nerve fiber layer thickness in the fellow eyes of normal-tension glaucoma patients with unilateral visual field defect. *Am J Ophthalmol*. 2005;140:165–166.

53. Susanna R, Jr., Galvao-Filho RP. Study of the contralateral eye in patients with glaucoma and a unilateral perimetric defect. *J Glaucoma*. 2000;9:34–37.

54. Medeiros FA, Sample PA, Weinreb RN. Frequency doubling technology perimetry abnormalities as predictors of glaucomatous visual field loss. *Am J Ophthalmol*. 2004;137:863–871.

55. Budenz DL, Anderson DR, Varma R, et al. Determinants of normal retinal nerve fiber layer thickness measured by Stratus OCT. *Ophthalmology*. 2007;114:1046–1052.

56. Wu Z, Huang J, Dustin L, Sadda SR. Signal strength is an important determinant of accuracy of nerve fiber layer thickness measurement by optical coherence tomography. *J Glaucoma*. 2009;18:213–216.

57. Pourhoseingholi MA, Baghestani AR, Vahedi M. How to control confounding effects by statistical analysis. *Gastroenterol Hepatol Bed Bench*. 2012;5:79–83.

58. Bender R, Lange S. Adjusting for multiple testing–when and how? *J Clin Epidemiol*. 2001;54:343–349.

translational vision science & technology